Received: 6 August 2019 | Revised: 22 September 2019 | Accepted: 16 October 2019
DOI: 10.1002/aoc.5364

FULL PAPER

WILEY Applied Organometallic Chemistry

# Pd nanoparticles supported on amphiphilic porous organic polymer as an efficient catalyst for aqueous hydrodechlorination and Suzuki-Miyaura coupling reactions

**Yizhu Lei[1] | Wenchao Zhu[1] | Yali Wan[2] | Renshu Wang[1] | Hailong Liu[1]**

[1] School of Chemistry and Materials Engineering, Liupanshui Normal University, Liupanshui, Guizhou 553004, China

[2] School of Chemistry and Chemical Engineering, Guizhou University, Guiyang, Guizhou 550025, China

**Correspondence**
Yizhu Lei, School of Chemistry and Materials Engineering, Liupanshui Normal University, Liupanshui. Guizhou, 553004, China.
Email: yzleiabc@126.com

**Funding information**
Academician Workstation of Liupanshui Normal University, Grant/Award Number: qiankehepingtairencai [2019]5604 hao; National Natural Science Foundation of China, Grant/Award Number: 21763017; Science and Technology Fund Project of Guizhou Province, Grant/Award Number: qian ke he ji chu [2018]1414] and[2016]1133; Scientific and Technological Innovation Platform of Liupanshui, Grant/Award Number: 52020-2018-03-02 and 52020-2017-02-02

Developing efficient and recyclable heterogeneous catalysts for organic reactions in water is important for the sustainable development of chemical industry. In this work, Pd nanoparticles supported on DABCO-functionalized porous organic polymer was successfully prepared through an easy copolymerization and successive immobilization method. Characterization results indicated that the prepared catalyst featured big surface area, hierarchical porous structure, and excellent surface amphiphilicity. We demonstrated the use of this amphiphilic catalyst in two case reactions, i.e. the aqueous hydrodechlorination and Suzuki-Miyaura coupling reactions. Under mild reaction conditions, the catalyst showed high catalytic activities for the two reactions. In addition, the catalyst could be easily recovered and reused for several times. Also, no obvious Pd leaching and aggregation of Pd nanoparticles occurred up during the consecutive reactions.

**KEYWORDS**
heterogeneous catalysis, hydrodechlorination, palladium nanoparticles, porous organic polymer, Suzuki-Miyaura coupling

## 1 | INTRODUCTION

With increasing consciousness for environmental protection, the use of water as a green reaction medium for replacing traditional organic solvents has gained considerable attention in recent years.[1,2] On the other hand, heterogeneous switching of homogeneous catalysis is considered as an important strategy for realizing environmentally benign organic transformations.[3–6] Therefore, there is good reason to believe that developing highly efficient catalyst for realizing aqueous and heterogeneous switching of homogeneous organic reactions would be an ideal pathway for green and sustainable organic synthesis. Nevertheless, organic transformations in water often suffer from poor reaction efficiency due to the high mass transfer resistance of hydrophobic organic substrates.[7,8] Thus, synthesis of water-compatible and efficient solid catalyst that allows low mass transfer resistance of the hydrophobic reactants in water is still a challenging task.[9,10] Over the past decades, many attempts have been made to address this challenging topic, while successful examples are limited to building

https://doi.org/10.1002/aoc.5364

emulsion systems,[11] and utilizing amphiphilic support.[9,10]

Pd nanoparticles with small diameters (1–10 nm) have been increasingly the focus of catalysis research in recent decades.[12–16] Due to the high surface-to-volume ratios and quantum size effects, Pd nanoparticles usually exhibited high catalytic activities in a variety of organic reactions.[12–16] However, these nanoparticles are thermodynamically unstable and easy to form Pd agglomerates because of their high surface energy. Generally, the aggregation of Pd nanoparticles leads to rapid decrease of the catalytic activities, and thus restricting their extensive applications. To this end, Pd nanoparticles supported on a variety of porous supports, such as zeolites,[17,18] porous carbons,[19,20] ordered mesoporous materials,[21] and metal–organic frameworks (MOFs),[22,23] have been attempted to resolve this issue. The results suggested that the porous supports could not noly enhance the stability of Pd nanoparticles, but also facilitate their recovery and reuse.

Porous organic polymers (POPs), which feature big surface areas and designable pore structures, have gained considerable attention recently as the solid supports to stabilize metal nanoparticles.[24–26] To date, a number of nitrogen and phosphine ligands functionalized POPs have been developed and used as the catalyst supports for palladium nanoparticles.[27–29] Due to the porous structure and nice electron-donating ability of the supports, these solid catalysts usually exhibited good aggregation and leaching resistant ability.[27–29] Nevertheless, the vast majority of POPs consist of hydrophobic aromatic frameworks, endowing the POPs with hydrophobic property, and thus, restricting their catalytic applications in water.[30–32] To resolve this problem, solid catalysts could be designed to be amphiphilic.[9,33–35] In recent years, investigations about the catalytic applications of metal nanoparticles supported on POPs have been widely reported, however, studies on amphiphilic POPs supported metal nanoparticles and their catalytic applications in water have rarely been explored.[30–32]

DABCO, a cage-like and small diazabicyclic molecule, has been widely used as an organocatalyst for various organic reactions.[36–38] Recently, we reported the first example of DABCO-functionalized porous organic polymer (P (DVB-DABCO)). As a heterogeneous organocatalyst, P (DVB-DABCO) exhibited excellent catalytic activity for the transesterification of glycerol with dimethyl carbonate.[39] In addition to being an organocatalyst, DABCO is also an efficient and inexpensive ligand for transition metals. In 2004, Li and coworkers[40] reported the first example of using DABCO as an efficient ligand for palladium-catalyzed Suzuki-Miyaura cross-coupling reaction. After that, DABCO-metal complexes have been widely used as catalysts for various Cross-Coupling reactions.[41–43] Although DABCO-metal complexes have been widely investigated, DABCO-functionalized porous organic polymer supported metal nanoparticles and their catalytic applications in water have never been investigated.

To develop efficient and heterogeneous palladium catalysts for organic reactions in water, we herein report the synthesis (Scheme 1) and catalytic applications of palladium nanoparticles supported on DABCO-functionalized porous organic polymer. The prepared catalyst featured big surface area, hierarchical porous structure, and excellent surface amphiphilicity. Under mild reaction conditions, the catalyst exhibited high catalytic activity, excellent aggregation resistant ability, and good reusability for aqueous hydrodechlorination and Suzuki-Miyaura coupling reactions.

## 2 | EXPERIMENTAL

### 2.1 | Materials

1,4-Diazabicyclo[2.2.2]octane (DABCO), Pd $(OAc)_2$, 4-vinylbenzyl chloride (90%), $NaBH_4$, aryl halides and aromatic boric acids were supplied by Energy Chemical. Divinylbenzene (DVB, 85%) was obtained from Alfa Aesar, washed repeatedly with NaOH solution (0.5 M) and deionized water before use. 2,2′-Azobis(2-methylpropionitrile) (AIBN) was purchased from Aladdin Chemistry and used as received. Vinyl functionalized DABCO monomer (DABCO monomer) was synthesized through the quaternization reaction of DABCO and 4-vinylbenzyl chloride, the detailed procedures was described in our previous report.[39]

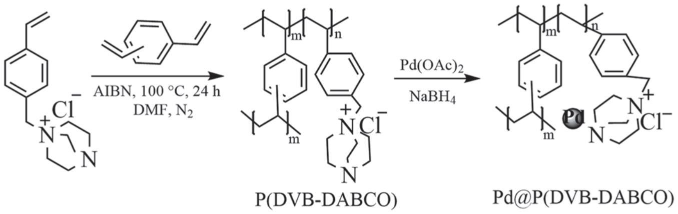

**SCHEME 1** Synthesis of Pd@P(DVB-DABCO) catalyst.

## 2.2 | Preparation of P (DVB-DABCO)

DABCO-functionalized porous organic polymer, P (DVB-DABCO), was prepared as our previous report.[39] In a typical procedure, divinylbenzene (1.2 g), DABCO monomer (0.8 g) and AIBN (50 mg) were dissolved in DMF (20 ml) in a Teflon autoclave (100 mL). Under nitrogen atmosphere, the autoclave was stirred at room temperature for 1 hr, then heated in a preheated oven at 100 °C for 24 hr. After the polymerization reaction, the resulting solid was extracted with ethanol and dried vacuum. Then, a pale-yellow solid was obtained and denoted as P (DVB-DABCO).

## 2.3 | Preparation of Pd@P (DVB-DABCO)

Generally, P (DVB-DABCO) (1.0 g) was added to a stirred solution of palladium acetate (0.044 g) in 30 ml ethanol, the resulting suspension was stirred at room temperature for 12 hr. Then, a solution of sodium borohydride (0.22 g) in 5 ml ethanol was added to the suspension dropwise and the resulting mixture was magnetically stirred for 2 hr. The resulting solid was separated by filtration, washed repeatedly with ethanol and deionized water, and then dried under vacuum. The obtained gray solid (1.0 g) was denoted as Pd@P (DVB-DABCO). The palladium loading of Pd@P (DVB-DABCO) was 2.0 wt% as determined by ICP analysis.

## 2.4 | Hydrodechlorination reaction

The hydrodechlorination reaction was carried out in a 10 ml reaction flask which fitted with $H_2$ balloon. Generally, Pd@P (DVB-DABCO) (21.2 mg, Pd: 0.004 mmol), aryl chloride (1 mmol), and NaOH (0.048 g, 1.2 mmol) were added to deionized water (4 ml). Then, the mixture was magnetically stirred at 25 °C under balloon of $H_2$. After the reaction, the resulting mixture was separated by centrifugation, the solid was extracted with ethanol for three times. The combined liquid was quantitatively by gas chromatography with biphenyl or *N,N*-dimethylformamide as an internal standard.

## 2.5 | Suzuki-Miyaura coupling reaction

Suzuki-Miyaura coupling reaction was conducted in a 10 ml reaction flask. In a typical procedure, Pd@P (DVB-DABCO) (26.5 mg, Pd:0.005 mmol), aryl halide (1 mmoml), arylboronic acid (1.5 mmol), and $K_3PO_4$■$3H_2O$ (2.0 mmol) were added to deionized water (4 ml). Then, the flask was stirred at 40 °C. After the reaction, the resulting mixture was separated by centrifugation, the recovered catalyst was extracted with ethanol for three times. For the model reaction, the combined liquid was quantitatively analyzed by gas chromatography with *N, N*-dimethylformamide as an internal standard. For investigation of the substrate scope, the combined liquid was purified using thin-layer chromatography with petroleum ether as the eluting solvent. Purity of the product was analyzed by $^1$H NMR. All of the obtained products are known compounds, and have been reported as our previously report.[32]

## 2.6 | Characterization

Nitrogen sorption isotherms of the samples was determined by a Micrometrics ASAP 2020 system at 77 K. FT-IR was analyzed on a Bruker Equinox 55 FT-IR spectrophotometer using KBr pellet technique at a 2 $cm^{-1}$ resolution. TEM image was obtained on a FEI Tecnai G2 F30 type microscope. SEM image was recorded on a Hitachi S-4800 type microscope. Palladium contents were measured using an ICP-PerkinElmer Optima 8000 instrument. XPS was recorded on a VG multilab 2000 spectrometer equipped with a Mg-AlKa X-ray source. Contact angle was measured on a Dataphysics OCA20 system. $^1$H NMR analysis was performed on a Bruker AVANCE III NMR spectrometer (400 MHz). Gas chromatography (GC) analysis was carried out on a Scientific™ TRACE™ 1310 (TRACE TR-WAX capillary column) with a FID detector.

# 3 | RESULTS AND DISCUSSION

## 3.1 | Characterization of the catalyst

As shown in Table 1, the results of Brunauer–Emmett–Teller (BET) analyses revealed that BET surface areas of

**TABLE 1** Physical properties of the P (DVB-DABCO) and Pd@P (DVB-DABCO)

| Entry | Catalysts | $S_{BET}$ ($m^2 \cdot g^{-1}$) | Pore volume ($cm^3$/g) [a] | Average pore radius (nm) [b] |
|---|---|---|---|---|
| 1 | P (DVB-DABCO) | 412 | 0.64 | 6.2 |
| 2 | Pd@P (DVB-DABCO) | 384 | 0.55 | 5.1 |

[a] Single point adsorption total pore volume of pores at $P/P_o = 0.95$.

[b] Adsorption average pore diameter (4 V/A by BET).

P (DVB-DABCO) and Pd@P (DVB-DABCO) were 412 and 384 $m^2 \cdot g^{-1}$, respectively. After supporting Pd nanoparticles, the surface area, pore volume and average pore radius of Pd@P (DVB-DABCO) decreased slightly. The decrease of these physical properties could be attributed to the partial pore filling with Pd nanoparticles.

Nitrogen adsorption–desorption isotherms of P (DVB-DABCO) and Pd@P (DVB-DABCO) were shown in Figure 1. The two samples displayed the combined sorption behavior of type I and type IV by IUPAC classification. The steep nitrogen gas uptake at low relative pressure ($P/P_0 < 0.01$) indicated the abundance of micropores, the slight hysteresis loops at $P/P_0 = 0.7–1.0$ regions implied the presence of mesopores; while the adsorption at medium to high pressure regions ($P/P_0 = 0.8–1.0$) suggested the presence of macropores. Pore size distribution curves (Figure 2) of P (DVB-DABCO) and Pd@P (DVB-DABCO) by NLDFT calculation method further demonstrated that the obtained samples had broad pore size distribution, comprising of micropores, mesopores and macropores. For solid catalyst, the abundant micropores facilitate the dispersion and stabilization of metal nanoparticles, while the big surface area and presence of mesopores and macropores in the solid catalyst could minimize diffusion barriers and enhance mass transport of the reactants.[24–29] Thus, it is reasonable to expect that the prepared solid catalyst would be a promising choice for heterogeneous catalyst due to its hierarchical porous structure and big surface area.

SEM characterization was used to analyze the morphology of the as-synthesized P (DVB-DABCO) and Pd@P (DVB-DABCO). It can be observed from Figure 3 a-b that P (DVB-DABCO) and Pd@P (DVB-DABCO) showed similar morphology, indicating that Pd@P (DVB-DABCO) retained very well morphology of the P (DVB-DABCO) support. TEM characterization was used to analyze the particle size of Pd nanoparticles in the Pd@P (DVB-DABCO) catalyst. As shown in Figure 3c-d, the TEM images of Pd@P (DVB-DABCO) showed that Pd nanoparticles was well distributed in the support with a relatively narrow size distribution. In Figure 3d, the average diameter of Pd clusters was about 2.8 nm.

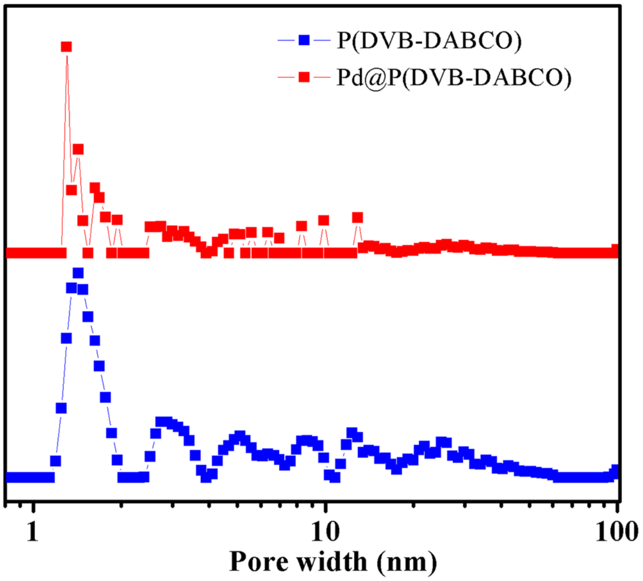

**FIGURE 2** Pore size distribution curves of P(DVB-DABCO) and Pd@P(DVB-DABCO) by NLDFT method

FT-IR spectra of P (DVB-DABCO) and Pd@P (DVB-DABCO) were shown in Figure 4. The results revealed

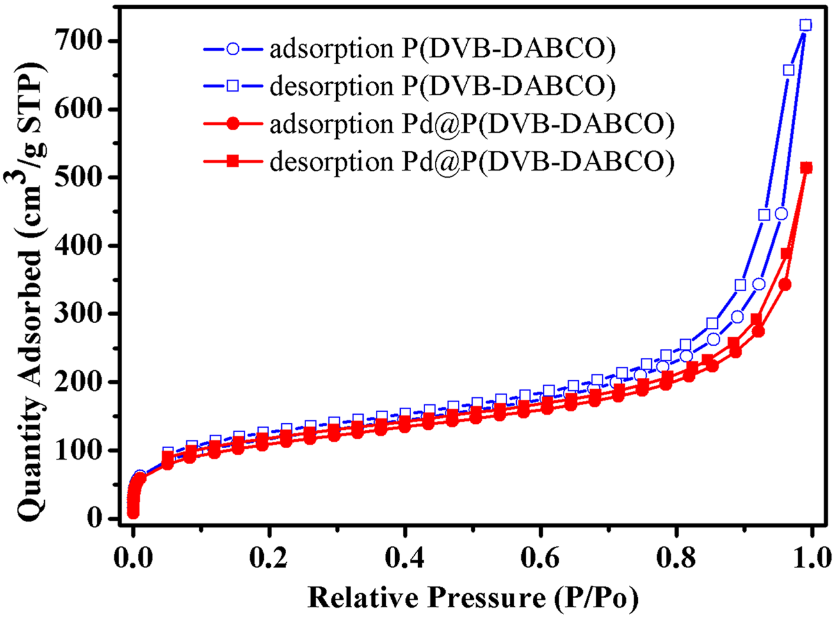

**FIGURE 1** Nitrogen adsorption (solid)-desorption (open) isotherms of P(DVB-DABCO) and Pd@P(DVB-DABCO)

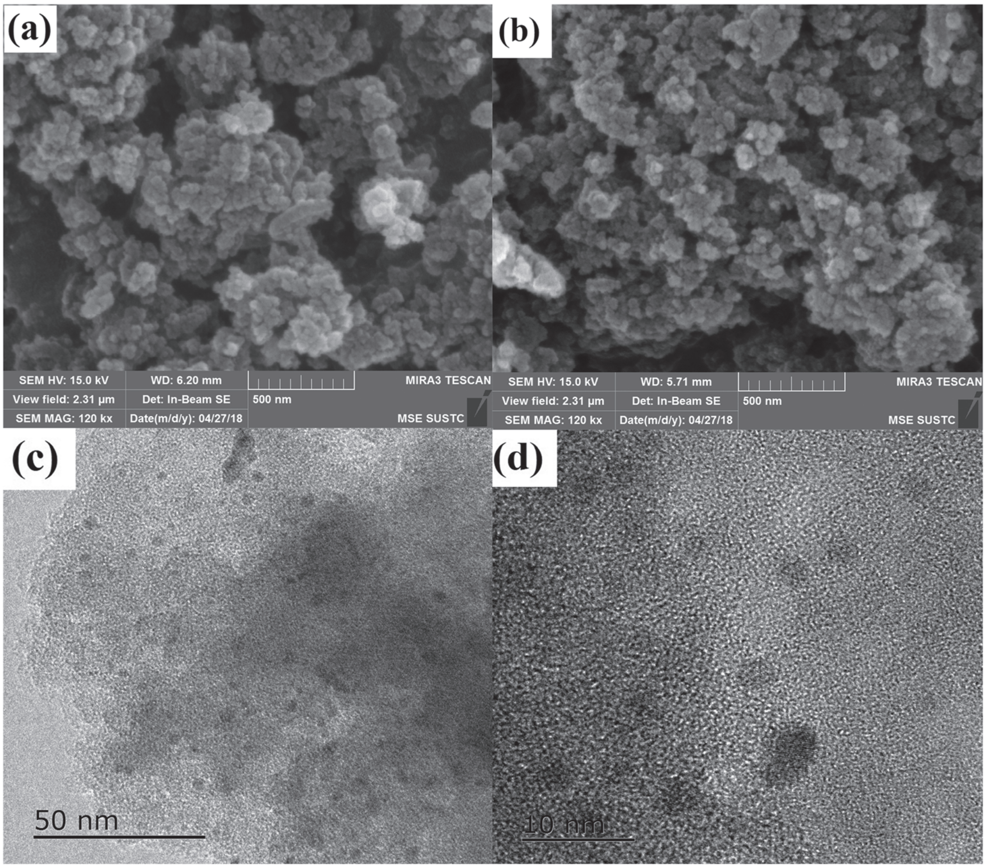

**FIGURE 3** SEM and TEM images of the samples. SEM images of (a) P(DVB-DABCO) and (b) Pd@P(DVB-DABCO); (c-d) TEM images of Pd@P(DVB-DABCO) at different magnification.

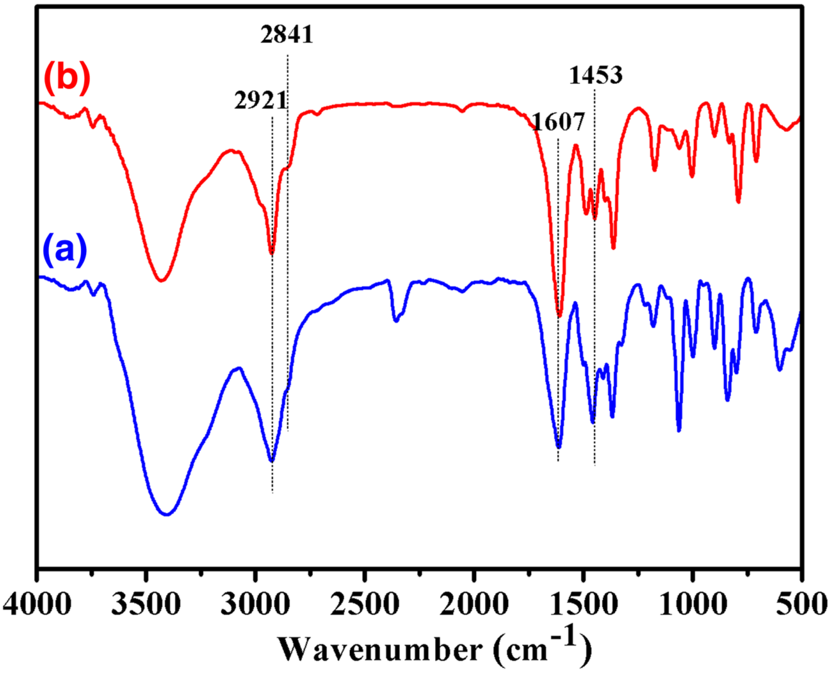

**FIGURE 4** FT-IR spectra of (a) P(DVB-DABCO) and (b) Pd@P(DVB-DABCO)

that P (DVB-DABCO) and Pd@P (DVB-DABCO) have almost the same characteristic peaks of infrared absorption (Figure 4, a and b), indicating no obvious structure change after Pd immobilization. The absorption peaks at 2921 and 2841 $cm^{-1}$ could be attributed to the stretching vibration of -$CH_2$ and -CH groups.[39] The peaks bands at

1607 and 1453 cm$^{-1}$ should be assigned to the C-C stretching vibration of aromatic ring.[39]

XPS studies were carried out to analyze the elemental compositions and electronic states of Pd species in the samples. As shown in Figure 5a, XPS full spectra of P (DVB-DABCO) and Pd@P (DVB-DABCO) validated the presence of N, C and Cl elements in the two samples. Besides, an additional Pd 3d band was observed for Pd@P (DVB-DABCO), suggesting the successful immobilization of palladium species in Pd@P (DVB-DABCO) catalyst. Pd 3d XPS spectrum in Figure 5b revealed that Pd species had the binding energies of 341.0 eV and 335.5 eV, corresponding to binding energies of Pd $3d_{3/2}$ and Pd $3d_{5/2}$, respectively. This indicated that Pd species in Pd@P (DVB-DABCO) was present in a zero state, thus proving the success reduction of Pd species in Pd@P (DVB-DABCO) catalyst.

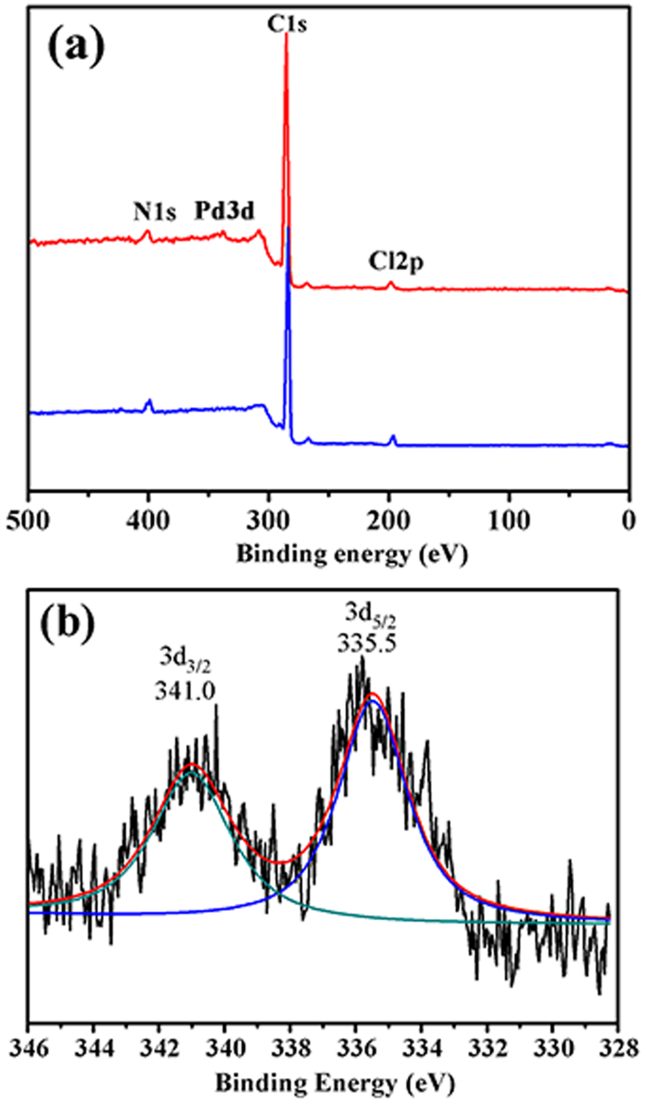

**FIGURE 5** (a) XPS full spectra of P(DVB-DABCO) and Pd@P(DVB-DABCO) (elemental scan); (b) Pd3d XPS spectrum of Pd@P(DVB-DABCO)

Previous results suggested that surface wettability of the solid catalysts has great influence on their catalytic performances in water.[9,30–35,44] To test the surface wettability of Pd@P (DVB-DABCO), contact angle measurements were carried out. For comparison, the contact angle of P (DVB-DABCO) towards water and methylbenzene was also tested. Figure 6a-b illustrated the contact angles of P (DVB-DABCO) and Pd@P (DVB-DABCO) for water. Interestingly, the water droplets were quickly absorbed by the two samples without any residue, suggesting the excellent hydrophilic properties of P (DVB-DABCO) and Pd@P (DVB-DABCO). Thus, the contact angles of the support and catalyst for water were recorded as 0°. Figure 6c-d illustrated the contact angles of P (DVB-DABCO) and Pd@P (DVB-DABCO) towards methylbenzene. Similarly, methylbenzene droplets were quickly absorbed by the two samples without any residue, suggesting their high lipophilicity. Experimental results of contact angle measurements revealed that the prepared Pd@P (DVB-DABCO) has excellent surface amphiphilicity. For solid catalyst in water, the excellent hydrophilicity enables the catalyst well disperse in water, while the excellent lipophilicity could enrich organic substrates in the porous framework of the catalyst, and thus accelerating the reaction rate.[30–32,44] Hence, it is not unreasonable to expect that the prepared solid could be a promising heterogeneous catalyst for catalyzing organic reactions in water due to its excellent surface amphiphilicity and porous structure.

## 3.2 | Hydrodechlorination of aryl chloride

The goal for preparation of porous and amphiphilic polymer supported nanopalladium is to develop efficient heterogeneous catalyst for aqueous organic reactions. With the expected material in hand, hydrodechlorination of aryl chloride, which is regarded as the most promising approach for the safe disposal of chlorinated organic pollutants in water,[45–47] was employed to investigate the catalytic performance of the obtained Pd@P (DVB-DABCO). Firstly, hydrodechlorination of 4-chlorophenol with $H_2$ was chosen as a model reaction to optimize the reaction conditions. The model reaction was carried out at room temperature under balloon pressure of $H_2$, the results were summarized in Table 2. To our delight, the reaction occurred smoothly at room temperature. With 0.5 mol% of Pd usage, a moderate conversion (60%) of 4-chlorophenol and yield (60%) of phenol were obtained within 3 hr using $Et_3N$ as a base (Table 2, entry 1). Under Ar atmosphere, no hydrodechlorination product was detected (Table 2, entry 2), suggesting the necessity of $H_2$. The reaction was also carried out in the absence of

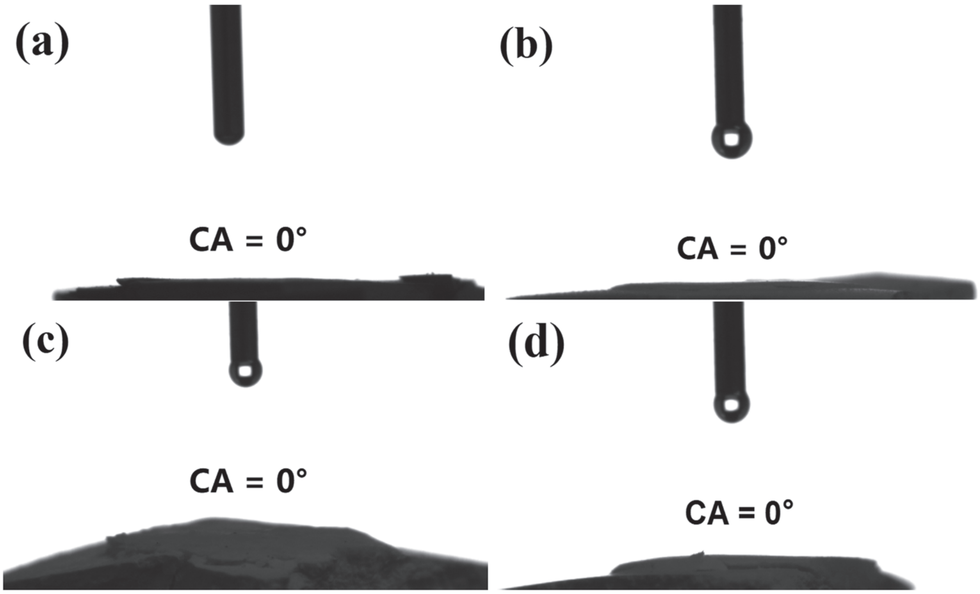

**FIGURE 6** Images of contact angle measurements for the samples. Photograph of a water droplet for (a) P(DVB-DABCO) and (b) Pd@P(DVB-DABCO), photograph of a methylbenzene droplet for (c) P(DVB-DABCO) and (d) Pd@P(DVB-DABCO)

**TABLE 2** Hydrodechlorination of 4-chlorophenol under various conditions[a]

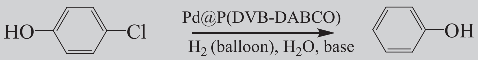

| Entry | Base | T (h) | Conv. (mol%)[b] | Yield (mol%)[b,c] | TOF[d] |
|---|---|---|---|---|---|
| 1 | $Et_3N$ | 3 | 60 | 60 | 40 |
| 2[e] | $Et_3N$ | 3 | - | - | - |
| 3 | - | 3 | 21 | 21 | 14 |
| 4 | DABCO | 3 | 79 | 79 | 53 |
| 5 | DBU | 3 | 72 | 70 | 47 |
| 6 | NaOH | 3 | >99 | >99 | 66 |
| 7 | $NaHCO_3$ | 3 | 33 | 33 | 22 |
| 8 | $Na_2CO_3$ | 3 | 84 | 84 | 56 |
| 9 | NaOH | 2 | 98 | 98 | 98 |
| 10 | NaOH | 1 | 87 | 86 | 172 |
| 11[f] | NaOH | 2 | 96 | 96 | 120 |
| 12[g] | NaOH | 2 | 84 | 84 | 140 |

[a] Reaction conditions: Pd@P (DVB-DABCO) (0.5 mol% Pd), $H_2$ (balloon), 4-chlorophenol (1.0 mmol), base (1.2 mmol), water (4 ml), 25 °C, stirring speed (800 rpm).

[b] GC yields.

[c] The total yields of phenol and sodium phenoxide.

[d] (mol product) $h^{-1}$ (mol Pd)$^{-1}$.

[e] Under balloon of Ar.

[f] Pd@P (DVB-DABCO) (0.4 mol% Pd).

[g] Pd@P (DVB-DABCO) (0.3 mol% Pd).

base, the result indicated that the absence of base diminished the catalytic efficiency (Table 2, entry 3). Considering the significant influence of base, different inorganic and organic bases were also tested (Table 2, entries 4–8). Among them, NaOH afforded the highest catalytic activity, and > 99% yield of hydrodechlorination product was

**TABLE 3** Comparison of Pd@P (DVB-DABCO) with the typical Pd-loaded catalysts for hydrodechlorination of 4-chlorophenol

| Entry | Catalyst (Pd, w%)[a] | Catal. usage[b] | Conditions | T (min) | Conv.(%) | Run | Ref. |
|---|---|---|---|---|---|---|---|
| 1 | Pd@P (DVB-DABCO) (2.0) | 21.2 mg (0.4 mol% Pd) | $H_2O$, 25 °C, 1 bar $H_2$ | 120 | 96 | 7 | Present work |
| 2 | Pd/h-m$SiO_2$ (2.5) | 20 mg | $H_2O$, 25 °C, 1 bar $H_2$ | 64 | 100 | 7 | [46] |
| 3 | Pd-IL/AC-cr (0.52) | 80.6 mg | $H_2O$, 33 °C, HCOONa/HCOOH | 120 | ~100 | 6 | [47] |
| 4 | $Fe_3O_4$@PPY@Pd (6.45) | 60 mg | $H_2O$, RT, ammonia borane | 120 | 92.5 | 5 | [48] |
| 5 | Pd/MSC (3.2) | 20 mg | MeOH, −15 °C, 1 bar $H_2$ | 600 | ~90 | not clearly mentioned | [49] |
| 6 | Pd/$SiO_2$-ODPA (3.5) | 2.5 mg | $H_2O$, 100 °C, 10 bar $H_2$ | 75 | 95 | 4 | [50] |
| 7 | PdNP@AT-mont. (8.14) | 40 mg | $H_2O$, 40 °C, 1 bar $H_2$ | 360 | 96 | 5 | [51] |
| 8 | Pd/clay (5) | 50 mg | $H_2O$, 30 °C, unclear | 300 | ~25 | 3 | [52] |
| 9 | $AgPd_4$/C | 0.4 mol% Pd | THF, RT, 1 bar $H_2$ | 240 | 98 | not clearly mentioned | [53] |

[a] Palladium loading of the solid catalyst.

[b] Catalyst usage (mg catal./mol substrate) or the palladium usage (Pd mole/substrate mole).

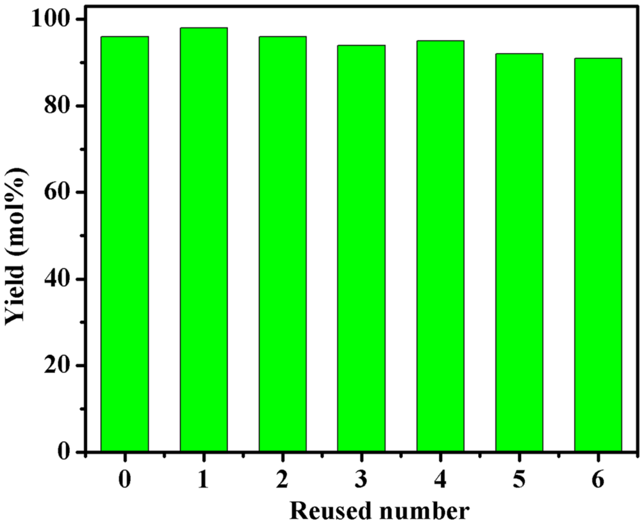

**FIGURE 7** Reuse of Pd@P(DVB-DABCO) for the hydrodechlorination of 4-chlorophenol. Reaction conditions: Pd@P(DVB-DABCO) (0.4 mol% Pd), H2 (balloon), 4-chlorophenol (1.0 mmol), NaOH (1.2 mmol), water (4 ml), 2 hr, 25 °C, stirring speed (800 rpm)

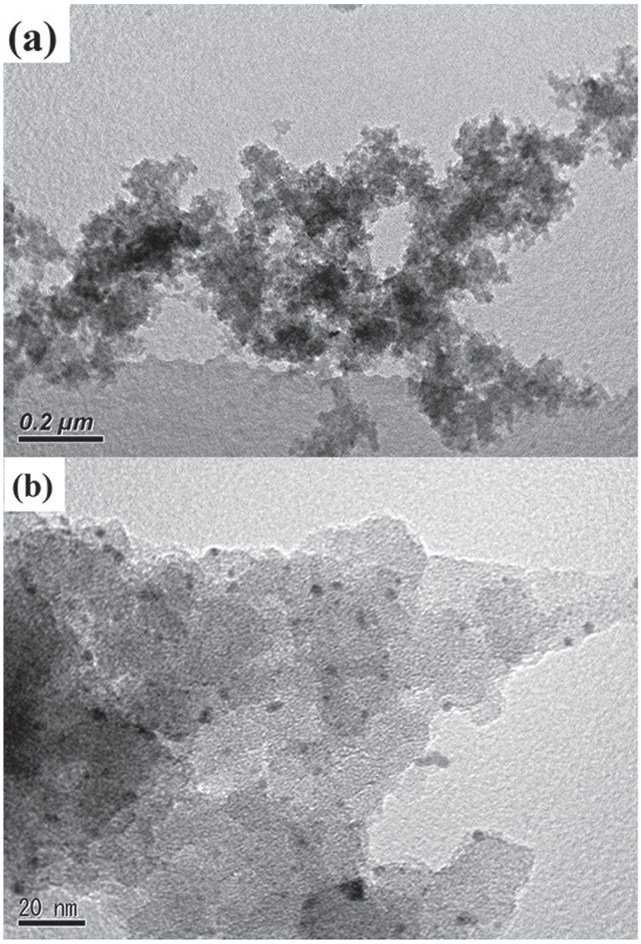

**FIGURE 8** TEM images of the 6th recycling Pd@P(DVB-DABCO) catalyst after the hydrodechlorination of 4-chlorophenol

**TABLE 4** Hydrodechlorination of various aryl chlorides with Pd@P (DVB-DABCO)[a]

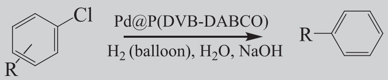

| Entry | R | T (h) | Conv. (mol%)[b] | Yield (mol%)[b] |
|---|---|---|---|---|
| 1 | *p*-Me | 2 | 93 | 93 |
| 2 | *m*-Me | 3 | 97 | 97 |
| 3 | *o*-Me | 3 | 91 | 91 |
| 4 | *p*-OMe | 3 | 98 | 98 |
| 5 | *p*-$NH_2$ | 2 | 99 | 99 |
| 6 | *p*-COMe | 2 | 93 | 91 |
| 7 | *p*-COOH | 2 | 99 | 99 |
| 8 | *p*-F | 2 | 95 | 95 |
| 9 | *p*-Ph | 2 | 82 | 82 |
| 10[c] | 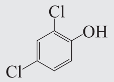 | 6 | 97 | 97 |

[a] Reaction conditions: Pd@P (DVB-DABCO) (0.4 mol% Pd), $H_2$ (balloon), 4-chlorophenol (1.0 mmol), NaOH (1.2 mmol), water (4 ml), 25 °C, stirring speed (800 rpm).

[b] GC yields.

[c] 2,4-dichlorophenol (0.5 mmol).

**TABLE 5** Effects of base and catalyst loading[a]

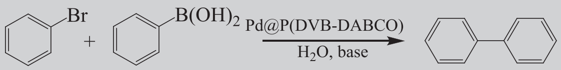

| Entry | Base | Catal. loading (mol%)[b] | Yield (mol%)[b] | TOF[c] |
|---|---|---|---|---|
| 1 | $K_2CO_3$ | 0.5 | 75 | 19 |
| 2 | $K_3PO_4$■$3H_2O$ | 0.5 | 92 | 23 |
| 3 | KOH | 0.5 | 53 | 13 |
| 4 | $Cs_2CO_3$ | 0.5 | 86 | 22 |
| 5 | $NaHCO_3$ | 0.5 | 37 | 9 |
| 6 | DABCO | 0.5 | 80 | 20 |
| 7 | DBU | 0.5 | 90 | 23 |
| 8 | $Et_3N$ | 0.5 | 68 | 17 |
| 9 | $K_3PO_4$■$3H_2O$ | 0.25 | 66 | 33 |
| 10 | $K_3PO_4$■$3H_2O$ | 0.1 | 21 | 26 |
| 11[d] | $K_3PO_4$■$3H_2O$ | 0.5 | 97 | 22 |
| 12[e] | $K_3PO_4$■$3H_2O$ | 0.5 | 95 | 24 |
| 13[e,f] | $K_3PO_4$■$3H_2O$ | 0.5 | 24 | 6 |

[a] Reaction conditions: Pd@P (DVB-DABCO) (0.5 mol%), bromobenzene (1.0 mmol), phenylboronic acid (1.5 mmol), base (2 mmol), water (4 ml), 40 °C, 8 hr, stirring speed (800 rpm).

[b] GC yields.

[c] (mol product) $h^{-1}$ (mol Pd)$^{-1}$.

[d] 9 hr.

[e] 25 °C, 15 hr.

[f] Pd@UPOP-1, 0.5 mol% Pd.

obtained (Table 2, entry 6). Then, the effect of reaction time and catalyst usage were investigated (Table 2, entries 9–12). Under the optimal reaction conditions, a 0.4 mol% of palladium catalyst usage was sufficient for high conversion (96%) of 4-chlorophenol within 2 hr, achieving a high TOF of 120 $h^{-1}$ (Table 2, entry 11). Thus, without any surfactants,[45] a highly active solid catalyst was obtained for the hydrodechlorination of 4-chlorophenol in water.

The comparison results of Pd@P (DVB-DABCO) with some typical Pd-loaded catalysts for the hydrodechlorination of 4-chlorophenol were listed in Table 3. The results indicated that the obtained Pd@P (DVB-DABCO) herein showed comparable[46] and higher catalytic activities than Pd-IL/AC-cr,[47] $Fe_3O_4$@PPY@Pd,[48] Pd/MSC,[49] Pd/$SiO_2$-ODPA,[50] PdNP@AT-mont.,[51] Pd/clay,[52] and $AgPd_4$/C.[53] This superior catalytic activity may be attributed to the porous and amphiphilic properties of Pd@P (DVB-DABCO), which benefit the mass transfer of 4-chlorophenol in water.

Then, recycling experiment of Pd@P (DVB-DABCO) was conducted. After the catalytic reaction, the recovered catalyst was washed with ethanol and water for three times. Then, the recycling solid was directly used for the next catalytic run. As shown in Figure 7, after reusing for six times, Pd@P (DVB-DABCO) was still capable of catalysing the hydrodechlorination of 4-chlorophenol in 91% yield, suggesting that the prepared Pd@P (DVB-DABCO) was quite robust under the reaction conditions. Pd content of the Pd@P (DVB-DABCO) after reusing 6 times was 1.97 wt% as determined by ICP. TEM images (Figure 8) of the recycled catalyst suggested that no significant change of morphology and no obvious aggregation of Pd nanoparticles occurred up during the recycling. These results further verified the robustness of the Pd@P (DVB-DABCO) catalyst. To conform the heterogeneous property of the catalyst, Pd leaching during the catalytic reaction was also studied. Pd@P (DVB-DABCO) catalysed hydrodechlorination of 4-chlorophenol was allowed to react for 1 hr firstly, the conversion of 4-chlorophenol reached to 77%. Then, the catalyst was filtered off. The resulting liquid mixture was added into another reaction tube and allowed to stir for 2 hr under balloon pressure of $H_2$. No conversion increase was observed after 2 hr. Besides, the Pd content in the liquid mixture was also measured by ICP, the result suggested that the Pd leaching was quite low, to be ca. 0.1 ppm, thus verifying the heterogeneity of the Pd@P (DVB-DABCO) catalyst.

Next, we tested the scope and generality of the catalytic system. Aryl chlorides bearing different functional groups were investigated, and the results were summarized in Table 4. *Para*-, *meta*- and *ortho*-methyl-substituted aryl chlorides reacted smoothly under the optimal reaction conditions, achieving high yields of dechlorinated products within 3 hr (Table 4, entries 1–3). It was also observed that *para*-substituted aryl chlorides with different electron-donating and electron-withdrawing groups were also well tolerated, affording moderate to excellent yields of dechlorinated products in 2 hr (Table 4, entries 4–9). Additionally, as a representative example of polyhalogenated substrate, 2,4-dichlorophenol was dechlorinated to 97% yield of phenol in 6 hr (Table 4, entry 10). Thus, this study offers an active and heterogeneous catalyst for the hydrodechlorination of aryl chloride in water.

## 3.3 | Suzuki–Miyaura coupling reaction

To further verify the catalytic performance of Pd@P (DVB-DABCO) in water, Suzuki-Miyaura coupling of aryl

**TABLE 6** Comparing the performance of different solid catalysts in the coupling of bromobenzene and phenylboronic acid

| Entry | Catalysts | Pd (mol%) | Conditions | T (h) | Yield(%) | Run | Ref. |
|---|---|---|---|---|---|---|---|
| 1 | Pd@P (DVB-DABCO) | 0.5 | $H_2O$, 40 °C | 9 | 97 | 6 | Present work |
| 2 | Phen-Pd-MOP | 0.6 | EtOH/$H_2O$, 80 °C | 0.5 | 99 | 12 | [54] |
| 3 | Phen-Pd-MOP | 0.6 | $H_2O$, 80 °C | 4 | 75 | 12 | [54] |
| 4 | Pd@UPOP-1 | 1 | $H_2O$, 25 °C | 18 | 99 | 5 | [32] |
| 5 | Pd/KAPs (DCM-TPP) | 1.29 | $H_2O$, 100 °C | 3 | 99 | 5 | [6] |
| 6 | Pd@PFN-P | 0.1 | EtOH/$H_2O$, 80 °C | 6 | 99.6 | 5 | [55] |
| 7 | $Fe_3O_4$@$SiO_2$@N,S-wG@Pd | 0.12 | EtOH/$H_2O$, 60 °C | 0.5 | 98 | 7 | [56] |
| 8 | PAA/PVA Nanofiber-NHC-Pd | 0.1 | $H_2O$, 80 °C | 8 | 80 | 5 | [57] |
| 9 | (NHC)Pd-rGO | 0.2 | EtOH, 75 °C | 2 | 98 | 6 | [58] |
| 10 | (1,4-$C_6H_4$)(GO-CPTMS@HPTPy-Pd-TPy)$_2$ | 1.38 | EtOH/$H_2O$, 80 °C | 3 | 92 | 4 | [59] |
| 11 | M-GO/(AM-MBA-$\beta$-CD@Pd) | 0.01 | $H_2O$, 50 °C | 3 | 91 | 7 | [60] |

halide, which is a typical coupling reaction,[8,16,32,42] was employed as the second case reaction. The coupling of phenylboronic acid with bromobenzene was chosen as a model reaction (Table 5). With 0.5 mol% of Pd usage, the influence of base was first investigated (Table 5, entries 1–8). Among the bases examined, $K_3PO_4$■$3H_2O$ afforded the highest catalytic activity, achieving 92% yield of biphenyl at 40 °C in 8 hr (Table 5, entry 2). Decreasing the Pd usage to 0.25 mol%, biphenyl was gained in 66% yield with a TOF of 33 $h^{-1}$ (Table 5, entry 9). Prolonging the reaction time to 9 hr, 97% yield of biphenyl was obtained (Table 5, entry 11). Interestingly, Pd@P (DVB-DABCO) was also quite efficient at 25 °C, and 95% yield of biphenyl could be gained in 15 hr (Table 5, entry 12). For comparison, palladium supported on urea-based amphiphilic porous organic polymer (Pd@UPOP-1), a heterogeneous catalyst for aqueous Suzuki–Miyaura coupling reaction that we reported recently,[32] was also tested under the same reaction conditions. However, only 24% yield of biphenyl was obtained (Table 5, entry 13).

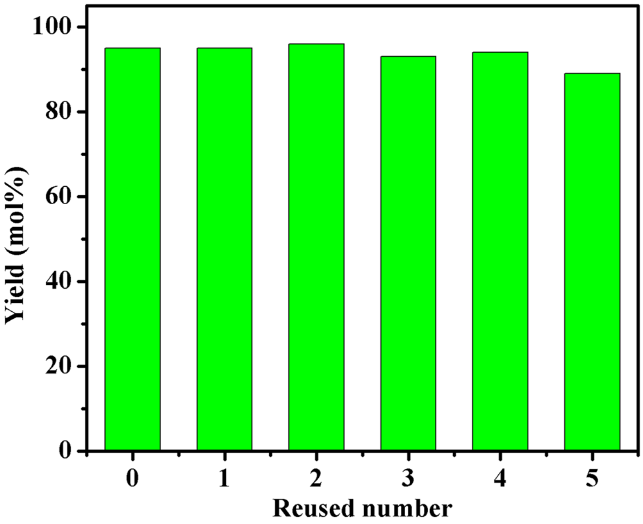

**FIGURE 9** Reuse of Pd@P(DVB-DABCO) for Suzuki-Miyaura coupling of bromobenzene and phenylboronic acid. Reaction conditions: Pd@P(DVB-DABCO) (0.5mol% Pd), bromobenzene (1.0 mmol), phenylboronic acid (1.5 mmol), K3PO4?3H2O (2 mmol), water (4 ml), 40 °C, 9 hr, stirring speed (800 rpm).

The comparison results of Pd@P (DVB-DABCO) with some recent heterogeneous catalysts for the coupling of bromobenzene and phenylboronic acid were also listed (Table 6). Under the mild reaction conditions, Pd@P (DVB-DABCO) showed moderate activity among the reported solid catalysts (Table 6, entries 2–12). Although Pd@P (DVB-DABCO) showed moderate catalytic activity for this coupling reaction, it should be noted that Pd@P (DVB-DABCO) is more in line with the requirements of

**TABLE 7** Suzuki–Miyaura coupling reaction catalysed by Pd@P (DVB-DABCO) [a]

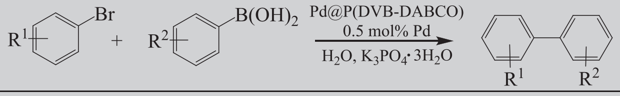

| Entry | $R^1$ | $R^2$ | Time (h) | Yield (%) [b] |
|---|---|---|---|---|
| 1 | *p*-Me | H | 9 | 94 |
| 2 | *m*-Me | H | 9 | 90 |
| 3 | *o*-Me | H | 12 | 94 |
| 4 | *p*-OMe | H | 15 | 88 |
| 5 | *p*-OH | H | 7 | 96 |
| 6 | *p*-COMe | H | 8 | 92 |
| 7 | *p*-CN | H | 8 | 94 |
| 8 | H | *p*-Me | 9 | 95 |
| 9 | H | *p*-OMe | 9 | 93 |
| 10 | H | *p*-CN | 9 | 96 |
| 11[c] | 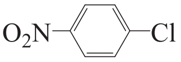 | H | 12 | 72 |
| 12[c] | 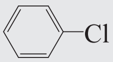 | H | 20 | 17 |

[a] Reaction conditions: Pd@UPOP-1 (0.5 mol% Pd), aryl bromide (1.0 mmol), arylboronic acid (1.5 mmol), $K_3PO_4 3H_2O$ (2.0 mmol), water (4 ml), 40 °C, stirring speed (800 rpm).

[b] Isolated yields.

[c] Aryl chlorides as the substrate.

green synthesis such as pure water reaction medium, mild reaction temperature, and facile preparation procedure.

Next, the recyclability of Pd@P (DVB-DABCO) catalyst was investigated over the coupling of phenylboronic acid with bromobenzene. After the completion of the model reaction, the recovered catalyst was washed with ethanol and water for three times, and then subjected to the next catalytic run. As depicted in Figure 9, the Pd@P (DVB-DABCO) catalyst could be effectively reused for five times with only a slight decrease of its activity. Thus, this result further verified the robustness of the prepared Pd@P (DVB-DABCO) in water-mediated reactions.

To investigate the scope and limitations of the Pd@P (DVB-DABCO) catalyst in Suzuki–Miyaura coupling reaction, aryl bromides and aryl boronic acids bearing different functional groups were tested. The results were summarized in Table 7. Firstly, the coupling reactions between substituted aryl bromides and phenylboronic were investigated (Table 7, entries 1–7). The results revealed that aryl bromides bearing both electron-withdrawing and electron-donating groups could react smoothly with phenylboronic, affording the corresponding biaryls in good to excellent yields within 15 hr. Then, the scope of arylboronic acids was also examined with several typical arylboronic acids (Table 7, entries 8–10). High yields of biaryls were gained in 9 hr regardless of the electronic property of the substituted groups. Chlorobenzene and 4-nitrochlorobenzene, as two representative substrates of aryl chlorides, were also tested under the optimal conditions. 72% yield of target biaryl was gained for 4-nitrochlorobenzene (Table 7, entry 11). However, only 17% yield of biphenyl was gained for chlorobenzene (Table 7, entry 12). All of these results revealed that the prepared Pd@P (DVB-DABCO) is an active and robust catalyst for water-mediated Suzuki–Miyaura coupling reaction of aryl bromides.

## CONCLUSIONS

In summary, DABCO-functionalized porous organic polymer supported nanopalladium catalyst was successfully prepared. The obtained catalyst featured big surface area, hierarchical porous structure, and excellent surface amphiphilicity. Under mild reaction conditions, the catalyst exhibited high catalytic activities for two organic reactions in water, i.e., the hydrodechlorination of aryl chlorides with $H_2$ and Suzuki–Miyaura coupling reaction of aryl bromides. Even at room temperature, two types of catalytic reactions can react smoothly. Moreover, the catalyst could be reused at least five times, and no obvious palladium leaching and aggregation of Pd nanoparticles occurred up during the consecutive reactions. In light of the easy preparation, good catalytic performance and excellent water stability of the present Pd@P (DVB-DABCO) catalyst, the results in this study would provide an efficient method and good reference for developing water-compatible heterogeneous nanometal catalysts.

## ACKNOWLEDGMENTS

This work is financial supported by the National Natural Science Foundation of China [grant number 21763017]; the Science and Technology Fund Project of Guizhou Province [grant number qian ke he ji chu [2018]1414] and[2016]1133]; the Scientific and Technological Innovation Platform of Liupanshui (52020-2018-03-02 and 52020-2017-02-02); the Academician Workstation of Liupanshui Normal University (qiankehepingtairencai [2019]5604 hao); and the Fund of Liupanshui Normal University (LPSSYZDXK201602).

## ORCID

*Yizhu Lei* https://orcid.org/0000-0002-9247-6000

## REFERENCES

[1] T. Kitanosono, K. Masuda, P. Xu, S. Kobayashi, *Chem. Rev.* **2018**, *118*, 679.

[2] U. M. Lindstrom, *Organic reactions in water: principles, strategies and applications*, Wiley-VCH, New York **2008**.

[3] C. Descorme, P. Gallezot, C. Geantet, C. George, *ChemCatChem* **2012**, *4*, 1897.

[4] M. Rose, *ChemCatChem* **2014**, *6*, 1166.

[5] B. Lai, R. Bai, Y. Gu, *ACS Sustainable Chem. Eng.* **2018**, *6*, 17076.

[6] J. Chen, J. Zhang, D. Zhu, T. Li, *Appl. Organometal. Chem.* **2018**, *32*, e3996.

[7] M. Zhang, L. Wei, H. Chen, Z. Du, B. P. Binks, H. Yang, *J. am. Chem. Soc.* **2016**, *138*, 10173.

[8] Y. Hao, X. Jiao, H. Zou, H. Yang, J. Liu, *J. Mater. Chem. A* **2017**, *5*, 16162.

[9] B. Lai, F. Mei, Y. Gu, *Chem. – Asian J.* **2018**, *13*, 2529.

[10] S. Pan, S. Yan, T. Osako, Y. Uozumi, *ACS Sus. Chem. Eng.* **2017**, *5*, 10722.

[11] Y. H. Hu, J. C. Wang, S. Yang, Y. A. Li, Y. B. Dong, *Inorg. Chem.* **2017**, *56*, 8341.

[12] J. K. Sun, Z. Kochovski, W. Y. Zhang, H. Kirmse, Y. Lu, M. Antonietti, J. Yuan, *J. am. Chem. Soc.* **2017**, *139*, 8971.

[13] Y. B. Huang, Q. Wang, J. Liang, X. Wang, R. Cao, *J. am. Chem. Soc.* **2016**, *138*, 10104.

[14] S. Doherty, J. G. Knight, T. Backhouse, E. Abood, H. Alshaikh, I. J. S. Fairlamb, R. A. Bourne, T. W. Chamberlain, R. Stones, *Green Chem.* **2017**, *19*, 1635.

[15] M. Gholinejad, F. Zareh, C. Nájera, *Appl. Organometal. Chem.* **2018**, *32*, e3984.

[16] A. R. Hajipour, A. R. Sadeghi, Z. Khorsandi, *Appl. Organometal. Chem.* **2018**, *32*, e4112.

[17] J. Zhang, L. Wang, B. Zhang, H. Zhao, U. Kolb, Y. Zhu, L. Liu, Y. Han, G. Wang, C. Wang, D. S. Su, B. C. Gates, F.-S. Xiao, *Nature Catal.* **2018**, *1*, 540.

[18] Y. Chai, S. Liu, Z. J. Zhao, J. Gong, W. Dai, G. Wu, N. Guan, L. Li, *ACS Catal.* **2018**, *8*, 8578.

[19] Y. Zhang, Z. Yin, H. Wang, X. F. Wu, *Org. Lett.* **2019**, *21*, 3242.

[20] A. Pourjavadi, Z. Habibi, *Appl. Organometal. Chem.* **2018**, *32*, e4480.

[21] M. Guo, H. Li, Y. Ren, X. Ren, Q. Yang, C. Li, *ACS Catal.* **2018**, *8*, 6476.

[22] A. Aijaz, Q. L. Zhu, N. Tsumori, T. Akita, Q. Xu, *Chem. Commun.* **2015**, *51*, 2577.

[23] M. Annapurna, T. Parsharamulu, P. Vishnuvardhan Reddy, M. Suresh, P. R. Likhar, M. Lakshmi Kantam, *Appl. Organometal. Chem.* **2015**, *29*, 234.

[24] P. Zhang, Z. A. Qiao, X. Jiang, G. M. Veith, S. Dai, *Nano Lett.* **2015**, *15*, 823.

[25] Q. Wang, X. Cai, Y. Liu, J. Xie, Y. Zhou, J. Wang, *Appl. Catal. B: Environ.* **2016**, *189*, 242.

[26] J. Mondal, Q. T. Trinh, A. Jana, W. K. H. Ng, P. Borah, H. Hirao, Y. Zhao, *ACS Appl. Mater. Interfaces* **2016**, *8*, 15307.

[27] R. Singuru, K. Dhanalaxmi, S. C. Shit, B. M. Reddy, J. Mondal, *ChemCatChem* **2017**, *9*, 2550.

[28] X. Wang, S. Min, S. K. Das, W. Fan, K. W. Huang, Z. Lai, *J. Catal.* **2017**, *355*, 101.

[29] Y. Wan, F. Song, T. Ye, G. Li, D. Liu, Y. Lei, *Appl. Organometal. Chem.* **2019**, *33*, e4714.

[30] Q. Sun, S. Ma, Z. Dai, X. Meng, F. S. Xiao, *J. Mater. Chem. A* **2015**, *3*, 23871.

[31] Y. Lei, Y. Wan, G. Li, X. Y. Zhou, Y. Gu, J. Feng, R. Wang, *Mater. Chem. Front.* **2017**, *1*, 1541.

[32] Y. Lei, G. Lan, D. Zhu, R. Wang, X. Y. Zhou, G. Li, *Appl. Organometal. Chem.* **2018**, *32*, e4421.

[33] M. Li, F. Wu, Y. Gu, *Chin. J. Catal.* **2019**, *40*, 1135.

[34] D. Yue, J. Lei, Z. Lina, G. Zhenran, X. Du, J. Li, *Catal. Lett.* **2018**, *148*, 1100.

[35] Y. Wan, Y. Feng, D. Wan, M. Jin, *RSC Adv.* **2016**, *6*, 109253.

[36] E. Safari, A. Hasaninejad, *ChemistrySelect* **2018**, *3*, 3529.

[37] J. Zhang, Y. Tang, W. Wei, Y. Wu, Y. Li, J. Zhang, Y. Zheng, S. Xu, *Org. Lett.* **2017**, *19*, 3043.

[38] H. Yang, R. Tian, Y. Li, *Front. Chem. China* **2008**, *3*, 279.

[39] Y. Wan, Y. Lei, G. Lan, D. Liu, G. Li, R. Bai, *Appl. Catal. A: Gen.* **2018**, *562*, 267.

[40] J.-H. Li, W.-J. Liu, *Org. Lett.* **2004**, *6*, 2809.

[41] J. H. Li, J. L. Li, D. P. Wang, S. F. Pi, Y. X. Xie, M. B. Zhang, X. C. Hu, *J. Org. Chem.* **2007**, *72*, 2053.

[42] S. Rostamnia, E. Doustkhah, B. Zeynizadeh, *Microp. Mesop. Mater.* **2016**, *222*, 87.

[43] S. Jadhav, S. Patil, A. Kumbhar, S. Kamble, R. Salunkhe, *Trans. Metal Chem.* **2019**, *4*, 1.

[44] L. Wang, F. S. Xiao, *Sci. China Mater.* **2018**, *61*, 1137.

[45] C. H. Lin, Y. H. Shih, J. MacFarlane, *Chem. Eng. J.* **2015**, *262*, 59.

[46] M. Tian, Y. Long, D. Xu, S. Wei, Z. Dong, *J. Colloid Interf. Sci.* **2018**, *521*, 132.

[47] R. Li, Z. Zhou, J. Chen, S. Wang, J. Zheng, C. Chu, J. Zhao, H. Fan, D. Han, *New J. Chem.* **2019**, *43*, 6659.

[48] X. Wei, X. Wan, J. Miao, R. Zhang, J. Zhang, Q. J. Niu, *Catal. Lett.* **2019**, *149*, 823.

[49] X. Li, Z. Jin, Q. Dai, X. Wang, *Res. Chem. Interm.* **2019**, *45*, 1087.

[50] T. Yoneda, *Chem. Lett.* **2018**, *47*, 945.

[51] P. K. Saikia, R. P. Bhattacharjee, P. P. Sarmah, L. Saikia, D. K. Dutta, *RSC Adv.* **2016**, *6*, 110011.

[52] P. Kar, B. G. Mishra, *J. Cluster Sci.* **2014**, *25*, 1463.

[53] H. Rong, S. Cai, Z. Niu, Y. Li, *ACS Catal.* **2013**, *3*, 1560.

[54] C. A. Wang, K. Nie, G. D. Song, Y. W. Li, Y. F. Han, *RSC Adv.* **2019**, *9*, 8239.

[55] G. Deng, Z. Wang, *Macromol. Rapid Commun.* **2018**, *39*, 1700618.

[56] S. Rohani, G. Mohammadi Ziarani, A. Badiei, *Appl. Organometal. Chem.* **2019**, e5142.

[57] B. Heidari, M. M. Heravi, M. R. Nabid, R. Sedghi, *Appl. Organometal. Chem.* **2019**, *33*, e4934.

[58] K. Karami, A. Ramezanpour, M. Zakariazadeh, C. Silvestru, *Appl. Organometal. Chem.* **2019**, *33*, e4907.

[59] K. Bahrami, H. Targhan, *Appl. Organometal. Chem.* **2019**, *33*, e4842.

[60] B. Heidari, M. M. Heravi, M. R. Nabid, R. Sedghi, S. E. Hooshmand, *Appl. Organometal. Chem.* **2019**, *33*, e4632.

**How to cite this article:** Lei Y, Zhu W, Wan Y, Wang R, Liu H. Pd nanoparticles supported on amphiphilic porous organic polymer as an efficient catalyst for aqueous hydrodechlorination and Suzuki-Miyaura coupling reactions. *Appl Organometal Chem*. 2019;e5364. https://doi.org/10.1002/aoc.5364